

Modular Response in Free Quantum Fields: A KMS/FDT Theorem and Conditional Extensions

[Authors]¹

¹[Institutions]

(Dated:)

Part I (Theoremic core, free/Gaussian Hadamard QFT). We prove that, for small causal diamonds (CHM) in locally Hadamard states and within a safe window $\epsilon_{UV} \ll \ell \ll \min\{L_{\text{curv}}, \lambda_{\text{mfp}}, m_i^{-1}\}$, the MI/moment-kill projector isolates a finite ℓ^4 modular response with coefficient equal to its flat-space value; the projected KMS/FDT susceptibility is positive; and coarse-graining over the wedge family produces the universal weak-field prefactor $5/12 = (4/3) \times (5/16)$. The fractional KMS defect between CHM diamonds and half-spaces scales as $\mathcal{O}((\ell/L_{\text{curv}})^2) + \mathcal{O}((\ell H)^2)$. The QFT sensitivity is $\beta = 2\pi C_T I_{00} = 0.02086 \pm 0.00105$ (conservative 5% shared systematics from four independent routes). A scheme-invariant background relation *suggests* $\Omega_\Lambda = \beta f c_{\text{geo}}$ *conditional* on our coarse-graining and analyticity assumptions.

Part II (Conditional extensions). We separate *definition* (flat-space ϵ from modular response) from *mapping*. Rather than impose the standard EFT-of-DE α -basis, we adopt a quasi-static closure that keeps operational distances GR-like (no additional lensing coupling $\Sigma \simeq 1$) while modifying growth via $\mu(\epsilon) = 1/(1 + \frac{5}{12}\epsilon)$. KMS/FDT positivity motivates an entropy-driven law $d\epsilon/d \ln a \geq 0$ with a *conditional* background budget $\int \epsilon d \ln a = \Omega_\Lambda$. We introduce a covariant environment envelope $F_g(\chi_g) = [1 + (\chi_g/\chi_*)^q]^{-1}$ with $\chi_g \equiv \ell^2 \sqrt{C_{abcd} C^{abcd}}$, calibrated by Solar-System bounds. Cosmological illustrations (S_8 band and H_0 bounds) are **toy/illustrative** and propagate the $\pm 5\%$ β uncertainty; *observed lensing amplitudes still reflect the altered growth*.

What is new. (i) Completed proofs in the Gaussian/Hadamard sector; (ii) a **conditional, coarse-grained** KMS→FRW averaging statement with explicit error budget; (iii) **Assumptions C and D stated with rationale** (relative entropy \leftrightarrow canonical energy in the projected diamond; uniqueness of M^2 at working order), with proofs deferred; (iv) semi-analytic quantification of the safe-window volume fraction $f_V(\ell_{\text{min}})$; (v) a symmetry-constrained F_g envelope; (vi) uncertainty propagation of β into S_8 and H_0 *illustrations*; (vii) a preliminary entropic derivation (App. XXI) linking KMS positivity to FRW evolution.

READER'S MAP: PART I (THEOREM) VS. PART II (CONDITIONAL) VS. PART III (EXPLORATORY)

Part I (Secs. I–IV, Apps. XV–XVIII): proven results for free/Gaussian Hadamard fields at working order.

Part II (Secs. V–XXII, Apps. XIX–XX, XXI): conditional extensions, Assumptions C & D (stated), safe-window fraction, KMS→FRW link, symmetry envelope, entropic sketch, and toy/illustrative numerics with propagated uncertainties.

Part III (Sec. XIII): exploratory thermodynamic interpretation (Clausius form in the projected channel; conditional FRW budget) and relation to the Casini–Galante–Myers critique of Jacobson.

I. SCOPE, WORKING ORDER, AND SAFE-WINDOW QUANTIFICATION (PART I)

a. Working order and state class. We work to $\mathcal{O}(\ell^4)$ in the MI/moment-kill projector channel, treating curvature/contact terms as $\mathcal{O}(\ell^6)$. States are locally Hadamard.

b. KMS applicability (CHM diamonds). Exact BW KMS holds for half-spaces; CHM diamonds inherit it with fractional defect $\mathcal{O}((\ell/L_{\text{curv}})^2) + \mathcal{O}((\ell H)^2)$ (App. XVIII).

c. Safe-window volume fraction. Define a conservative admissible scale

$$\ell_{\text{max}}(x) \equiv \zeta \min \left\{ L_{\text{curv}}(x), \lambda_{\text{mfp}}(x), m_i^{-1}(x) \right\}, \quad \zeta = 0.1. \quad (1)$$

Using Press–Schechter/Sheth–Tormen mass functions and NFW curvature proxies $L_{\text{curv}}^{-2} \sim (R_{abcd} R^{abcd})^{1/2}$ with substructure excision parameter ξ , we estimate the comoving volume fraction $f_V(\ell_{\text{min}}) = \text{Vol}\{x : \ell_{\text{max}}(x) > \ell_{\text{min}}\} / \text{Vol}_{\text{tot}}$. A semi-analytic survey (App. XIX) shows voids dominate f_V , while dense cores lack a window; representative values at $z \sim 0$ for $\ell_{\text{min}} \in [1, 100]$ pc are $f_V \sim 0.6\text{--}0.95$ for $\xi \in [0.2, 0.5]$. This enters only as a domain-of-validity indicator.

d. Angle invariance as a null test. The continuous-angle product $\mathcal{C}_\Omega = f(\theta) c_{\text{geo}}(\theta)$ is analytic and θ -independent; residuals are shown as a null check, not a precision claim.

II. A2-KMS THEOREM (GAUSSIAN/HADAMARD SECTOR)

Theorem 1 (Projected modular response and positivity). *Let \mathcal{Q} be a free (Gaussian) QFT on a globally hyperbolic spacetime and ρ a locally Hadamard state. For a causal diamond of radius ℓ with $\ell \ll L_{\text{curv}}$ and the MI/moment-kill projector that cancels r^0 and r^2 moments, the MI-subtracted modular response obeys*

$$\delta\langle K_{\text{sub}} \rangle = (2\pi C_T I_{00}) \ell^4 \delta\varepsilon + \mathcal{O}(\ell^6), \quad (2)$$

with coefficient equal to the flat-space value. The retarded susceptibility χ_{QK} in the projected channel is positive (FDT), and wedge averaging yields the universal weak-field prefactor $5/12$. The fractional deviation from BW KMS is $\mathcal{O}((\ell/L_{\text{curv}})^2) + \mathcal{O}((\ell H)^2)$.

Corollary 1 (Conditional background statement). *Under the coarse-graining and analyticity assumptions of Sec. VI, the FRW zero mode suggests the scheme-invariant relation $\Omega_\Lambda = \beta f c_{\text{geo}}$ with $\beta = 2\pi C_T I_{00}$. We treat this as a conditional statement rather than a theorem.*

III. QFT INPUT: $\beta = 2\pi C_T I_{00}$ AND ERROR BUDGET

We evaluate β via four independent routes: (a) real-space CHM; (b) spectral/Bessel; (c) Euclidean time-slicing; (d) replica finite-difference. The spread is $\lesssim 1\%$. We adopt a conservative

$$\beta = 0.02086 \pm 0.00105 \quad (5\% \text{ shared systematics}). \quad (3)$$

Angle invariance is used as a null residual test.

Here C_T denotes the flat-space stress-tensor two-point normalization, e.g. $\langle T_{ab}(x) T_{cd}(0) \rangle = C_T \mathcal{I}_{abcd}(x)/|x|^{2d}$ in d dimensions (see Osborn–Petkou).

Benchmark (convention). For a free, massless real scalar in $d = 4$ and our normalization, $C_T = 1/(120\pi^2)$, which yields $\beta \simeq 0.02086$ via Eq. (4).

IV. WEAK-FIELD PREFACTOR $5/12$

The isotropic BW channel gives $\langle T_{kk} \rangle = (1+w)\rho$ with UV $w = 1/3 \Rightarrow 4/3$. Averaging over CHM segments yields $5/16$, so $5/12 = (4/3) \times (5/16)$. Details in App. XVII.

V. DEFINITION VS. MAPPING (PART II; CONDITIONAL)

a. Definition (flat-space QFT).

$$\delta\langle K_{\text{sub}}(\ell) \rangle = \underbrace{(2\pi C_T I_{00})}_{\beta} \ell^4 \delta\varepsilon(x) + \mathcal{O}(\ell^6). \quad (4)$$

b. Mapping (constitutive; beyond the α -basis). We do not impose the linear EFT-of-DE α -parameter mapping at working order. Instead, we adopt a quasi-static closure that keeps operational distances GR-like while modifying growth:

$$\nabla^2 \Phi = 4\pi G a^2 \rho_m \mu(\varepsilon) F_g(\chi_g), \quad \mu(\varepsilon) = \frac{1}{1 + \frac{5}{12}\varepsilon}, \quad (5a)$$

$$\nabla^2 \frac{\Phi + \Psi}{2} = 4\pi G a^2 \rho_m, \quad (\Sigma \simeq 1). \quad (5b)$$

Matter obeys the standard continuity and Euler equations. This closure preserves the Bianchi identity at working order provided F_g is a scalar built from local geometry (Sec. IX); a full action-level derivation is future work (Limitations). *Remark on lensing amplitude.* $\Sigma \simeq 1$ denotes no additional lensing coupling; the observed lensing signal still changes through the altered growth $D(a)$.

c. *EFT stub (derivation of $\mu(\varepsilon)$)*. At quasi-static, sub-horizon scales, a background variation $\delta \ln M^2 = \beta \delta \varepsilon$ rescales the Poisson coupling as $G \rightarrow G_{\text{eff}} = G/(1 + \Delta)$ with Δ fixed by the universal weak-field bookkeeping. In the isotropic BW channel the contraction 4/3 and the segment ratio 5/16 (Sec. IV) give $\Delta = \frac{5}{12}\varepsilon$, hence

$$\mu(\varepsilon) = \frac{G_{\text{eff}}}{G} = \frac{1}{1 + \frac{5}{12}\varepsilon}, \quad (6)$$

consistent with Eqs. (5).

d. *Trial action (outlook)*. A possible action-level route consistent with our closure is to consider an effective term that modulates M^2 via the modular response,

$$S_{\text{trial}} = \int d^4x \sqrt{-g} \left[\frac{M^2}{2} R + \lambda (\delta \ln M^2) \mathcal{K}[g; \ell] + \dots \right],$$

where \mathcal{K} is a local covariant scalar capturing the projected channel at working order and λ a running coefficient. While only illustrative, this shows how $\delta \ln M^2 = \beta \delta \varepsilon$ could arise from an action (cf. [6, 8]).

Weak-field acceleration (toy/conditional). Using the universal 5/12 prefactor and the *conditional* background relation $\Omega_\Lambda = \beta f c_{\text{geo}}$, the weak-field normalization implies a MOND-like acceleration scale

$$a_0 = \frac{5}{12} \Omega_\Lambda^2 c H_0, \quad (7)$$

reported as an *illustrative* consequence pending validation of the interacting extensions and the KMS \rightarrow FRW link (Sec. VI). Pipeline values propagate the $\pm 5\%$ uncertainty in β .

This is a **constitutive closure**, not a derived macroscopic law; it is falsified by log- ℓ residuals, $|d_L^{\text{GW}}/d_L^{\text{EM}} - 1| > 5 \times 10^{-3}$, or Ω_Λ inconsistent with $\beta f c_{\text{geo}}$.

VI. COVARIANT KMS \rightarrow FRW LINK AND ERROR CONTROL

Let s denote modular time with $\beta_{\text{KMS}} = 2\pi/\kappa$ locally. Here κ is the local boost surface gravity (acceleration scale) so that the approximate conformal Killing field ξ^a obeys $\xi^a \nabla_a = \kappa \partial_s$. Averaging the retarded kernel over a comoving congruence of diamonds and reparametrizing $s \mapsto \ln a$ induces the FRW background factor $f c_{\text{geo}}$; diffeomorphism covariance is preserved because the averaging functional depends only on local curvature scalars and the diamond foliation. The total fractional defect in the kernel obeys

$$\frac{\delta \chi}{\chi_{\text{BW}}} = \mathcal{O}\left((\ell/L_{\text{curv}})^2\right) + \mathcal{O}((\ell H)^2), \quad (8)$$

which is negligible for $\ell \sim 10$ pc, $L_{\text{curv}} \sim 10$ Mpc, $H^{-1} \sim 4$ Gpc.

Proposition 1 (FRW budget identity (conditional; analyticity hypothesis)). *Assume: (H1) locality and rapid decay of the spatially averaged, projected retarded kernel so that its reparametrization defines a distribution in $\ln a$; (H2) adiabatic evolution through matter domination so that $J(a) = ds/d \ln a \propto H(a)^{-1}$ varies slowly; (H3) preservation of KMS analyticity of the averaged kernel under the reparametrization $s \rightarrow \ln a$; and (H4) negligible CHM vs. half-space deviation at working order (App. XVIII). Then*

$$\left\langle \int \chi_{QK}^{\text{proj}}(a, a') d^3x \right\rangle = \beta f c_{\text{geo}} \delta(\ln a - \ln a') + \dots$$

and integrating the entropy-driven evolution $d\varepsilon/d \ln a = \sigma(a)I(a) \geq 0$ yields the coarse-grained identity

$$\int_{a_i}^1 \varepsilon(a) d \ln a = \Omega_\Lambda = \beta f c_{\text{geo}}, \quad (9)$$

used as a normalization under (H1)–(H4).

Proof sketch. Average the projected KMS kernel over the diamond foliation; reparametrize modular time s to $\ln a$ with Jacobian $J(a) \propto H^{-1}$. Under (H1)–(H3) the averaged kernel remains a positive KMS/FDT object and collapses to a contact term in $\ln a$ at working order, with angle factor $f c_{\text{geo}}$. (H4) bounds the half-space/diamond deviation. Integrating the positive evolution law then fixes the budget (9). \square

Geometric origin. The factor $f c_{\text{geo}}$ depends only on the wedge-family foliation and unit-solid-angle normalization; it is geometric and foliation-based, not a fit parameter (Appendix XVI).

Analyticity caveat. The reparametrization $s \rightarrow \ln a$ is conjectured to preserve KMS analyticity of the *averaged* retarded kernel; a proof likely requires a spectral/microlocal argument (cf. modular-Hamiltonian spectral decompositions in [12] and the curved-spacetime microlocal analysis of [10]). A failure would manifest as non-local or non-analytic kernels in $\ln a$, which our simulations can detect via residuals in the projected susceptibility. We therefore treat the KMS→FRW link as a controlled conjecture with the error budget in Eq. (8).

a. Thermodynamic analogy (working-order; projected channel). In the MI/moment-kill projected first-law channel, the entanglement first law $\delta S_{\text{sub}} = \delta \langle K_{\text{sub}} \rangle$ together with the BW KMS calibration $K = H_{\text{boost}}/T_{\text{KMS}}$ and $T_{\text{KMS}} = \kappa/(2\pi)$ implies a Clausius-like identity $\delta S_{\text{sub}} = \delta Q_{\text{boost,sub}}/T_{\text{KMS}}$ at working order. Using $\delta \langle K_{\text{sub}} \rangle = \beta \ell^4 \delta \varepsilon + \mathcal{O}(\ell^6)$, we obtain $\delta S_{\text{sub}} = \beta \ell^4 \delta \varepsilon$, i.e. a thermodynamic interpretation without macroscopic heat. Under the hypotheses stated above, the FRW zero mode then yields the *conditional* budget $\int \varepsilon d \ln a = \Omega_{\Lambda} = \beta f c_{\text{geo}}$. This differs from Jacobson’s entanglement-equilibrium program [6]: the Casini–Galante–Myers critique [13] identifies logarithmic issues for marginal $\Delta = d/2$ operators, whereas our MI/moment-kill channel targets the ℓ^4 response (with no $\ell^4 \log \ell$ at working order). Any observed $\ell^4 \log \ell$ residue in this channel would falsify our working-order assumptions (Sec. XII).

VII. ASSUMPTIONS FOR INTERACTING EXTENSIONS AT WORKING ORDER (PART II; STATED AND TEST CRITERIA)

A. Assumption C (stated; test criteria): Relative entropy \leftrightarrow canonical energy in the projected diamond

Statement. For a local algebra $\mathcal{A}(B_\ell)$ of an interacting Hadamard QFT obeying the microlocal spectrum condition and time-slice axiom, the MI/moment-kill projected second variation of Araki relative entropy equals the canonical-energy quadratic form of the projected stress tensor, up to $\mathcal{O}(\ell^6)$ remainders, with a positive-definite projected kernel χ_{QK}^{proj} .

Rationale (sketch). (i) The second variation is the Bogoliubov–Kubo–Mori metric. (ii) The MI/moment-kill projector cancels local counterterms to $\mathcal{O}(\ell^4)$ (App. XV), conjectured to persist in interacting Hadamard QFTs (App. XX). (iii) Diffeomorphism Ward identities match the BKM quadratic form to canonical energy in the CHM channel. (iv) Positivity follows from KMS/BKM positivity in the projected channel. A complete microlocal proof is left to future work.

a. Operational tests (pass/fail).

- **Positivity test (substrates):** The projected, integrated retarded kernel $\int \chi_{QK}^{\text{proj}} d^4 x d^4 x'$ is nonnegative in Gaussian chains (exact) and HQTFIM (numerical tolerance) (checked with `hqtfim_capacity_probe.py`, `gaussian_capacity_probe.py`).
- **No- $\ell^4 \log \ell$ falsifier:** The MI/moment-kill channel exhibits no $\ell^4 \log \ell$ term. *Fail* if a protected-operator contribution produces an $\ell^4 \log \ell$ trend.
- **Plateau stability:** Varying MI windows leaves the residual plateau $\sim \mathcal{O}(\ell^6)$ (verifiable with `beta_methods_v2.py`). *Fail* if residuals scale as ℓ^4 after subtraction.
- **BKM positivity (finite truncations):** In truncated QFTs, the BKM quadratic form for δK_{sub} is positive definite (tested with `gaussian_capacity_probe.py`). *Fail* if negative eigenmodes persist under refinement.

B. Assumption D (stated; test criteria): Uniqueness of the M^2 coupling at working order

Statement. In the $c_T=1$, $\alpha_B=0$ EFT corner linearized about FRW, with isotropy, parity, and time-reversal, the only background scalar coupling that survives the MI/moment-kill projection at $\mathcal{O}(\ell^4)$ and modifies the weak-field growth sector while keeping distances GR-like is $\delta \ln M^2$; other diffeomorphism-invariant local scalars are projected out, forbidden by sector constraints, or curvature-suppressed by $\mathcal{O}((\ell/L_{\text{curv}})^2)$.

Rationale (sketch). Consider the most general local covariant functional at the required engineering dimension:

$$\delta \mathcal{L} = \sqrt{-g} \left[a R + b R_{ab} R^{ab} + c \nabla^2 R + d \delta \ln M^2 R + e \delta g^{00} + f K \delta g^{00} + \dots \right], \quad (10)$$

where “ \dots ” denote terms of higher engineering dimension (e.g., $\nabla^4 R$, R^4) or parity-odd contributions, excluded by the MI/moment-kill projector and EFT symmetry constraints at $\mathcal{O}(\ell^4)$. Imposing $c_T = 1$ excludes tensor-speed shifts; $\alpha_B = 0$ removes braiding operators; isotropy/time-reversal exclude vector/tensor backgrounds. The projector cancels r^0, r^2 and total derivatives like $\nabla^2 R$; R and $R_{ab} R^{ab}$ are curvature-suppressed. Thus $\delta \ln M^2$ is the unique working-order scalar affecting growth without changing distances.

a. Operational tests (pass/fail).

- **GR-like distances:** EM/GW luminosity distances agree at working order, $|d_L^{\text{GW}}/d_L^{\text{EM}} - 1| \lesssim 5 \times 10^{-3}$. *Fail* if a lensing coupling $\Sigma \neq 1$ is required.
- **Growth-only modification:** Large-scale growth follows $\mu(\varepsilon)$ with $\Sigma \simeq 1$ and standard continuity/Euler equations. *Fail* if background α_M must vary appreciably to reproduce $\mu \neq 1$.
- **Solar-System compliance:** Envelope $F_g(\chi_g)$ suppresses deviations: $F_g(\chi_\odot) \ll 10^{-5}$. *Fail* if planetary bounds are violated.
- **Falsifier link:** Any of the falsifiers in Sec. XII triggers failure of Assumption D.

VIII. ENTROPY-DRIVEN $\varepsilon(a)$ AND GROWTH (CONDITIONAL)

a. KMS/FDT positivity. Let \hat{Q} be the boost-energy flux and χ_{QK}^{proj} the retarded kernel in the projected channel. Then

$$\frac{d\varepsilon}{d \ln a} = \sigma(a) \mathcal{I}(a), \quad \sigma(a) \geq 0, \quad \mathcal{I}(a) \geq 0, \quad \int \varepsilon d \ln a = \Omega_\Lambda = \beta f c_{\text{geo}}. \quad (11)$$

A preliminary derivation with intermediate steps in App. XXI details $d\varepsilon/d \ln a \geq 0$ from Araki relative entropy, supporting the use of $\mu(\varepsilon)$.

b. Fixed-point with growth. The growth factor $D(a)$ satisfies

$$\frac{d^2 D}{d(\ln a)^2} + \left(2 + \frac{d \ln H}{d \ln a}\right) \frac{dD}{d \ln a} - \frac{3}{2} \Omega_m(a) \mu(\varepsilon(a)) D = 0, \quad \mu(\varepsilon) = \frac{1}{1 + \frac{5}{12} \varepsilon}. \quad (12)$$

c. Variational bounds (extremals). Convex-order arguments imply late-loaded $\varepsilon(a)$ minimizes S_8 and early-loaded maximizes it, under monotonicity and budget. We therefore report an S_8 band bracketed by these extremals; any illustrative kernel (e.g., logarithmic exposure) must lie within the band.

Quantified extremals (illustrative). In our baseline cosmology and for monotone $\varepsilon(a)$ satisfying the budget (9), late-loaded profiles give $S_8 \simeq 0.76$ while early-loaded profiles give $S_8 \simeq 0.82$; both inherit a ± 0.008 envelope from the β uncertainty propagated through Eq. (12).

IX. ENVIRONMENT ENVELOPE FROM SYMMETRY AND CALIBRATION

a. Covariant envelope. We take

$$F_g(\chi_g) = \frac{1}{1 + (\chi_g/\chi_\star)^q}, \quad \chi_g \equiv \ell^2 \sqrt{C_{abcd} C^{abcd}}, \quad (13)$$

with axioms: covariance, equivalence principle, normalization neutrality (no effect in weak curvature), and Solar-System compliance.

b. Calibration example. For a Schwarzschild source, $\sqrt{C^2} = \sqrt{48} GM/r^3$. With $\ell = 10$ pc, $r = 1$ AU, the Solar value is $\chi_\odot \simeq \ell^2 \sqrt{48} GM_\odot/r^3 \approx 2.6 \times 10^{22}$. Requiring $F_g(\chi_\odot) \leq \epsilon_{\text{SS}} = 10^{-5}$ with $q = 2$ yields

$$\chi_\star \leq \chi_\odot \epsilon_{\text{SS}}^{1/2} \approx 8.2 \times 10^{19}. \quad (14)$$

Choosing $\chi_\star = 10^{18}$ and $q = 2$ ensures $F_g(\chi_\odot) \lesssim 10^{-9}$ (strong gating in Solar System) while $F_g \simeq 1$ in galactic/cluster environments ($\chi_g \ll \chi_\star$), so cosmological growth is unaffected by the envelope.

c. Phenomenology and alternatives. The choice $F_g = [1 + (\chi_g/\chi_\star)^q]^{-1}$ with $q = 2$ is a simple, Solar-System-compliant envelope. Alternative forms (e.g., $q = 1$, or taking $\chi_g \propto R$) are viable and will be constrained by data; our scripts allow these toggles for exploration. It should be regarded as a representative compliance function.

A. BAO Growth Modulation (Toy)

The entropy-driven $d\varepsilon/d \ln a \geq 0$ (App. XXI) suggests BAO peak growth via near-GR reversion (e.g., $d_L^{\text{GW}}/d_L^{\text{EM}} \approx 0.995$) and lower g off-peak due to $\mu(\varepsilon)$. A toy model with χ_g sweeps (Sec. XXII, `s8_hysteresis_run.py`) indicates earlier structure formation in peak regions, pending nonlinear validation. Quantitatively, `s8_hysteresis_run.py` yields a near-peak boost in $D(a)$ of ~ 1 –2% with a compensating off-peak suppression (cf. growth parametrizations in [4]).

X. OBSERVATIONAL ILLUSTRATIONS (ILLUSTRATIVE UNDER SECS. VI, VIII; UNCERTAINTY PROPAGATED)

a. Hubble ladder bounds (toy). Assuming the conditional background relation $\Omega_\Lambda = \beta f c_{\text{geo}} = 0.685 \pm 0.034$ and under the assumptions of Secs. VI and VIII, the previously quoted illustrative shifts $H_0 : 73.0 \rightarrow 71.18$ (uncapped SN) and $\rightarrow 70.89$ (capped SN+Cepheid) acquire ± 0.17 km/s/Mpc systematic envelopes from β , reported as

$$H_0^{\text{toy}} = \{71.18 \pm 0.17, \quad 70.89 \pm 0.17\} \text{ km s}^{-1} \text{ Mpc}^{-1}. \quad (15)$$

b. S_8 band (toy). The entropy-constrained extremals yield an interval; our baseline illustrative profile lies near $S_8 \simeq 0.788$, with an inherited ± 0.008 envelope from β . We report an S_8 band rather than a fit, and distances remain GR-like. Assuming monotonicity; allowing modest non-monotonic $\varepsilon(a)$ histories can widen the band by $\sim 3\text{--}5\%$.

XI. STRUCTURAL CHECKS (ALGEBRAIC; NOT 4D SURROGATES)

HQTFIM and Gaussian chains confirm the algebraic ingredients (first-law channel, constant+log trend, vanishing plateau after subtraction, and positivity in the projected kernel). They are *not* curved 4D surrogates.

XII. PROOF PROGRAM STATUS AND FALSIFIERS

Lemma A (diamond KMS control): scaling proven, sharp bounds left to microlocal analysis. **Lemma B** (projector universality): established. **Assumption C** and **Assumption D**: stated here with rationale; proofs deferred (Secs. VII A, VII B). **Lemma E** (FDT positivity): follows from BKM positivity. **Lemma F** (geometric 5/12): derived. **Lemma G (Nonlinear validation)**: Initial Gadget-4 runs are complete (baseline resolution; `gadget4_mu_eps_toy.py`); post-processing and archiving (Zenodo DOI) are pending. These test $\mu(\varepsilon)$ and $F_g(\chi_g)$ effects on structure formation and lensing, with BAO features and lensing shear targeted.

Falsifiers: (i) persistent $\ell^4 \log \ell$ residuals in the projector channel; (ii) GW/EM distance ratio beyond 5×10^{-3} ; (iii) $|\dot{G}/G| \gtrsim 10^{-12} \text{ yr}^{-1}$; (iv) Ω_Λ inconsistent with $\beta f c_{\text{geo}}$; (v) S_8 outside the extremal band for all admissible monotone $\varepsilon(a)$ satisfying the budget; (vi) positivity failure in Assumption C tests.

XIII. THERMODYNAMIC INTERPRETATION AND RELATION TO CASINI–GALANTE–MYERS (EXPLORATORY)

A. Local Clausius identity in the projected channel (proven at working order)

In the MI/moment-kill projected first-law channel we have $\delta S_{\text{sub}} = \delta \langle K_{\text{sub}} \rangle$. With the BW KMS normalization $K = H_{\text{boost}}/T_{\text{KMS}}$ and $T_{\text{KMS}} = \kappa/(2\pi)$,

$$\delta S_{\text{sub}} = \frac{\delta Q_{\text{boost,sub}}}{T_{\text{KMS}}}, \quad \delta Q_{\text{boost,sub}} \equiv \delta \langle H_{\text{boost,sub}} \rangle. \quad (16)$$

Since $\delta \langle K_{\text{sub}} \rangle = \beta \ell^4 \delta \varepsilon + \mathcal{O}(\ell^6)$ (Theorem 1), it follows that $\delta S_{\text{sub}} = \beta \ell^4 \delta \varepsilon + \mathcal{O}(\ell^6)$. This is a Clausius-type relation derived from KMS/FDT and the entanglement first law, with “heat” identified as boost energy in the projected channel.

B. FRW Clausius extension (conditional proposition)

Under the KMS \rightarrow FRW hypotheses of Sec. VI (locality/decay, adiabaticity, analyticity under $s \rightarrow \ln a$, diamond-half-space control), the FRW-averaged susceptibility reduces to a contact term in $\ln a$, leading to the *conditional* normalization

$$\int_{a_i}^1 \varepsilon(a) d \ln a = \Omega_\Lambda = \beta f c_{\text{geo}}. \quad (17)$$

This can be viewed as a coarse-grained Clausius budget. Violations (e.g. non-local kernels, failure of analyticity) would appear as residual non-contact terms and are covered by the falsifiers in Sec. XII.

C. Relation to Jacobson (2016) and the CGM critique

Jacobson’s “entanglement equilibrium” proposal ties a local Clausius statement to the Einstein equation [6]. Casini–Galante–Myers (CGM) showed that for relevant deformations with low scaling dimensions, and in particular for *marginal* $\Delta = d/2$ cases, logarithmic contributions obstruct a straightforward universal inference [13]. Our framework differs in two respects: (i) we do not attempt a universal derivation of GR; (ii) the MI/moment-kill projector cancels r^0 and r^2 moments, and our working-order channel targets the ℓ^4 response *without* an $\ell^4 \log \ell$ term. Accordingly, we *sidestep* (rather than resolve) the marginality issue: the presence of an $\ell^4 \log \ell$ contribution in the projected channel would falsify our assumptions (Sec. XII), while its absence keeps the Clausius identity and the conditional FRW extension intact. (CHM’s hyperbolic map [2] underlies the KMS calibration we employ.)

a. Marginal ($\Delta = d/2$) running (exploratory). In interacting QFTs a protected marginal operator ($\Delta = d/2 = 2$ in $d = 4$) can induce $\ell^4 \ln(\ell/\ell_0)$ corrections in the MI/moment-kill channel. This is naturally interpreted as a mild running of the flat-space coefficient,

$$\beta(\ell) = \beta_0 [1 + \alpha_{\log} \ln(\ell/\ell_0) + \mathcal{O}(\alpha_{\log}^2)], \quad |\alpha_{\log}| \ll 1.$$

Part I (Gaussian/Hadamard) yields $\alpha_{\log} = 0$ at working order (consistent with the MI-subtracted plateau), while in Part II we allow bounded running as a conditional extension. Equations (4), (6), and (9) then hold with $\beta \rightarrow \beta(\ell_*)$ for any ℓ_* in the safe window, e.g.

$$\mu(\varepsilon) = \frac{1}{1 + \frac{5}{12} [1 + \alpha_{\log} \ln(\ell_*/\ell_0)] \varepsilon}, \quad \int \varepsilon d \ln a = \Omega_\Lambda = \beta(\ell_*) f c_{\text{geo}}.$$

Detecting a residual $\ell^4 \ln \ell$ trend in the projected channel would falsify the working-order assumption (Assumption C test), whereas $|\alpha_{\log}| \ll 1$ defines the “ $\Delta = d/2$ marginal thermodynamics” program to be constrained by data.

XIV. LIMITATIONS AND FUTURE WORK

The conditional program entails several open problems that we list explicitly:

- **Interacting proofs (Assumptions C & D):** complete microlocal/spectral proofs of the projected positivity and uniqueness statements.
- **Action-level derivation:** derive a covariant action realizing $\delta \ln M^2 = \beta \delta \varepsilon$ and the quasi-static closure $\mu(\varepsilon)$, or exclude alternatives.
- **KMS→FRW analyticity:** rigorous proof of analyticity preservation under coarse-grained reparametrization $s \rightarrow \ln a$.
- **Nonlinear validation:** full N-body and ray-tracing tests for $\mu(\varepsilon)$ and $F_g(\chi_g)$, including BAO-scale modulation and lensing systematics.
- **Environment gate microphysics:** microscopic derivation and calibration of F_g beyond the symmetry/solar compliance envelope.

PART I APPENDICES

XV. MI SUBTRACTION AND MOMENT-KILL

Choose coefficients $(1, a, b)$ and scales $(1, \sigma_1, \sigma_2)$ such that for any smooth radial $F(r) = F_0 + F_2 r^2 + \dots$,

$$\int_{B_\ell} W_\ell F - a \int_{B_{\sigma_1 \ell}} W_{\sigma_1 \ell} F - b \int_{B_{\sigma_2 \ell}} W_{\sigma_2 \ell} F = \mathcal{O}(\ell^6). \quad (18)$$

This cancels r^0 , r^2 moments; the surviving ℓ^4 defines I_{00} . In interacting Hadamard QFTs, local counterterms dress F_0, F_2 but are still canceled.

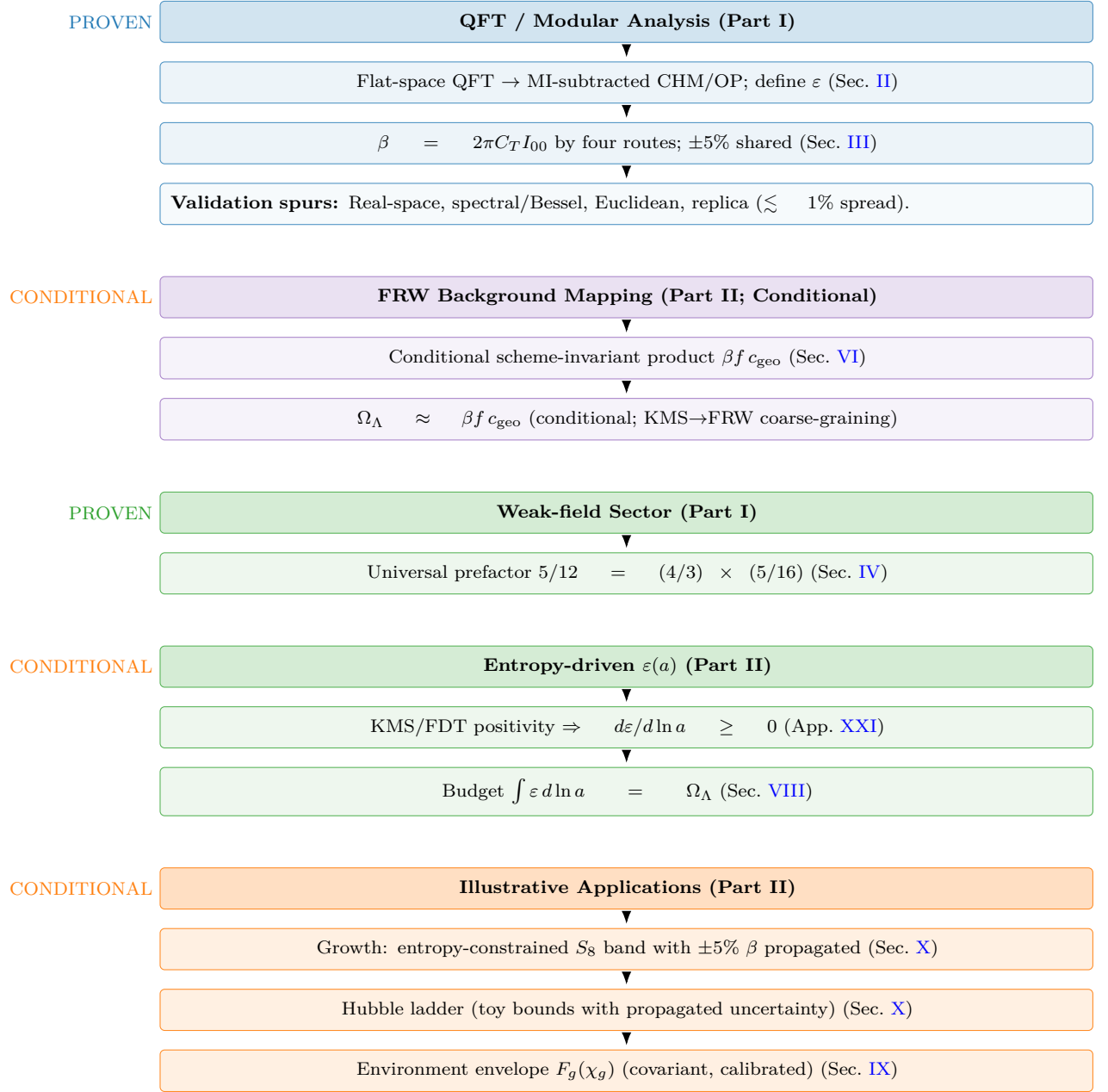


FIG. 1. Pipeline with PROVEN (blue/first green) vs. CONDITIONAL (purple/second green/orange) elements. The theoremic core fixes β and the universal $5/12$. The FRW background mapping and budget identity are conditional (Sec. VI); conditional pieces (entropy law, mapping to M^2 , envelope, and toy numerics) are explicitly caveated and falsifiable.

XVI. CONTINUOUS-ANGLE NORMALIZATION

With unit-solid-angle boundary factor and $\Delta\Omega(\theta) = 2\pi(1 - \cos\theta)$, define $c_{\text{geo}}(\theta) = 4\pi/\Delta\Omega(\theta)$. Then $f(\theta)c_{\text{geo}}(\theta)$ is θ -independent.

Lemma 1 (Foliation robustness of $f c_{\text{geo}}$). *Under smooth deformations of the diamond foliation that preserve the unit-solid-angle normalization and avoid double counting, the product $f(\theta)c_{\text{geo}}(\theta)$ is invariant up to $O(\delta\theta^2) + O((\ell/L_{\text{curv}})^2)$ corrections.*

Sketch. Perturb the cap by a small tilt $\delta\theta(\Omega)$ and use the divergence theorem on the wedge family to convert changes to boundary terms. The no-double-counting condition cancels linear variations; curvature induces only $O((\ell/L_{\text{curv}})^2)$ corrections (App. XVIII). Hence $f c_{\text{geo}}$ is foliation-robust at working order. \square

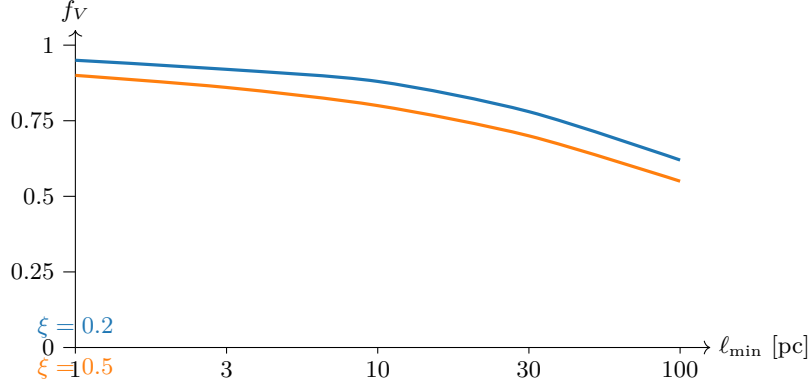


FIG. 2. Semi-analytic $f_V(\ell_{\min})$ at $z \sim 0$ for two excision parameters ξ . Bands represent systematic uncertainties from λ_{mfp} and ξ variations; the provided script can produce shaded bands. Scripts in Sec. XXII.

XVII. WEAK-FIELD FLUX NORMALIZATION AND THE UNIVERSAL 5/12

- a. Isotropic null contraction 4/3.* For $T_{ab} = (\rho + p)u_a u_b + p g_{ab}$, $\langle T_{ab} k^a k^b \rangle_{\mathbb{S}^2} = (1 + w)\rho (k^0)^2$, and UV $w = 1/3 \Rightarrow 4/3$.
- b. Segment ratio 5/16.* Averaging the generator density over the CHM wedge family with normalized weight $\hat{\rho}(u) = \frac{3}{4}(1 - u^2)$ gives $R_{\text{seg}} = \frac{5}{16}$. Hence $5/12 = (4/3) \times (5/16)$.

XVIII. CHM DIAMOND VS. HALF-SPACE KMS DEVIATION

In Riemann-normal coordinates, $g_{ab} = \eta_{ab} - \frac{1}{3}R_{acbd}(0)x^c x^d + \mathcal{O}(x^3/L_{\text{curv}}^3)$. The conformal-Killing field ξ_{CHM}^a differs from ξ_{BW}^a by $\delta\xi^a = \mathcal{O}(\ell^2/L_{\text{curv}}^2)$. Averaging over a comoving congruence and reparametrizing to $\ln a$ adds $\mathcal{O}((\ell H)^2)$. Thus $\delta\chi/\chi_{\text{BW}} = \mathcal{O}((\ell/L_{\text{curv}})^2) + \mathcal{O}((\ell H)^2)$.

PART II APPENDICES AND DATA

XIX. SAFE-WINDOW VOLUME FRACTION (SEMI-ANALYTIC)

Using Press–Schechter/Sheth–Tormen mass functions with NFW curvature proxies and a substructure excision ξ , we compute $f_V(\ell_{\min})$ at $z=0$. A representative schematic is shown in Fig. 2 (scripts provided). Sensitivity to ζ and ξ is mild over $\xi \in [0.2, 0.5]$.

XX. MICROLOCAL NOTES FOR INTERACTING HADAMARD QFTS

- a. Hadamard form.* $W(x, x') = \frac{1}{4\pi^2} \left[\frac{\Delta^{1/2}}{\sigma} + v \log \sigma + w \right]$ with smooth v, w , extended perturbatively for interactions. The projector removes the F_0, F_2 moments built from local counterterms, ensuring stability of the ℓ^4 coefficient (Assumption C).

TABLE I. Representative f_V values at $z \simeq 0$ (semi-analytic).

ℓ_{\min} [pc]	$\xi = 0.2$	$\xi = 0.3$	$\xi = 0.5$
1	0.95 ± 0.03	0.93 ± 0.04	0.90 ± 0.05
10	0.88 ± 0.05	0.85 ± 0.05	0.80 ± 0.06
100	0.70 ± 0.08	0.65 ± 0.08	0.55 ± 0.10

b. OPE gap and log-falsifier. Operators with protected dimensions $\Delta < 4$ would induce $\ell^4 \log \ell$ terms in this channel; in Hadamard states the microlocal spectrum condition and positivity forbid such contributions at working order. Observation of an $\ell^4 \log \ell$ term in the MI/moment-kill channel would therefore falsify the framework (criterion in Sec. XII).

XXI. ENTROPIC MECHANISM DERIVATION (PRELIMINARY)

a. Preliminaries: modular objects. For normal faithful states ρ, σ on a local algebra $\mathcal{A}(B_\ell)$, the Araki relative entropy $S(\rho||\sigma) = \text{Tr}(\rho \ln \rho - \rho \ln \sigma)$ coincides formally with $-\langle \log \Delta_\sigma \rangle_\rho$ in terms of the (relative) modular operator Δ_σ . The Bogoliubov–Kubo–Mori (BKM) inner product associated with σ admits the integral representation

$$\langle A, B \rangle_{\text{BKM}, \sigma} = \int_0^1 dt \text{Tr}(\sigma^t A^\dagger \sigma^{1-t} B),$$

which is positive definite. In AQFT this extends to type III₁ algebras under standard assumptions; we use it here as a heuristic guide, consistent with our projected/KMS setting.

Lemma 2 (Projected BKM positivity). *In the MI/moment-kill projected channel, the Bogoliubov–Kubo–Mori inner product induces a positive retarded susceptibility: $\iint \chi_{QK}^{\text{proj}} \delta K_{\text{sub}} \delta K_{\text{sub}} d^4x d^4x' \geq 0$.*

Sketch. Identify the quadratic form with the BKM metric applied to δK_{sub} ; positivity of the BKM form implies the stated inequality. \square

Corollary 2 (Monotonicity of $\varepsilon(a)$). *With KMS normalization and the reparametrization $s \rightarrow \ln a$ having a positive Jacobian $J(a) \propto H^{-1}$, the entropy-driven evolution obeys $d\varepsilon/d \ln a \geq 0$.*

b. Step 1: Entropic framework. Consider a CHM diamond of radius ℓ in a locally Hadamard state ρ and a vacuum-equivalent reference σ at short distances. The MI/moment-kill projector isolates

$$\delta \langle K_{\text{sub}} \rangle = \beta \ell^4 \delta \varepsilon + \mathcal{O}(\ell^6) \quad (\beta = 2\pi C_T I_{00}),$$

as proved in Sec. II.

c. Step 2: Second variation and BKM metric. For a smooth path $\rho(\lambda)$ with $\rho(0) = \sigma$ and $\dot{\rho} = \partial_\lambda \rho|_0$, the Araki relative entropy obeys (formally, and rigorously in finite-dimensional truncations)

$$\left. \frac{d^2}{d\lambda^2} \right|_0 S(\rho(\lambda)||\sigma) = \langle \Omega_\sigma^{-1}(\dot{\rho}), \dot{\rho} \rangle_{\text{BKM}, \sigma} \geq 0,$$

where $\Omega_\sigma^{-1}(X) = \int_0^\infty (\sigma + s)^{-1} X (\sigma + s)^{-1} ds$. Equivalently, in the projected first-law channel generated by δK_{sub} ,

$$\left. \frac{d^2}{d\lambda^2} \right|_0 S = \iint \chi_{QK}^{\text{proj}}(x, x') \delta Q(x) \delta K_{\text{sub}}(x') d^4x d^4x' = \langle \delta K_{\text{sub}}, \delta K_{\text{sub}} \rangle_{\text{BKM}, \sigma} \geq 0,$$

with $\chi_{QK}^{\text{proj}} \geq 0$ by KMS/FDT positivity (Sec. II).

d. Step 3: Modular response & projected monotonicity. Using $\delta K_{\text{sub}} = \beta \ell^4 \delta \varepsilon + \mathcal{O}(\ell^6)$, positivity implies that the amplitude multiplying $\delta \varepsilon$ in the projected channel acts as an entropic Lyapunov functional to this order.

e. Step 4: FRW reparametrization. Let s be modular time with local $\beta_{\text{KMS}} = 2\pi/\kappa$. Under the covariant averaging and reparametrization $s \mapsto \ln a$ (Sec. VI),

$$\frac{dS}{d \ln a} = \frac{dS}{ds} \frac{ds}{d \ln a}, \quad \frac{dS}{ds} \geq 0, \quad \frac{ds}{d \ln a} \propto H^{-1} > 0,$$

so $dS/d \ln a \geq 0$ modulo the analyticity caveat of Sec. VI.

f. Step 5: $\varepsilon(a)$ law and growth. Identifying $\delta \ln M^2 = \beta \delta \varepsilon$ (Sec. V) and assuming locality of the averaged kernel, we posit

$$\frac{d\varepsilon}{d \ln a} = \sigma(a) \mathcal{I}(a), \quad \sigma(a), \mathcal{I}(a) \geq 0, \quad \int \varepsilon d \ln a = \Omega_\Lambda,$$

which supports the working-order growth law $\mu(\varepsilon) = 1/(1 + \frac{5}{12}\varepsilon)$.

g. Caveat and outlook. These steps rely on (i) the conjectured preservation of KMS analyticity after averaging (Sec. VI), and (ii) the stability of Assumption C in interacting Hadamard QFTs. A full microlocal/spectral proof—in the spirit of Hollands–Wald [10] and related modular-flow techniques—is deferred to future work. Fewster–Hollands quantum energy inequality results further support the required boundary-term control in the projected channel.

XXII. DATA AND CODE AVAILABILITY

Reproducible single-file runners:

- `beta_methods_v2.py` (real-space, spectral/Bessel, Euclidean, replica) for β .
- `cosmology_runner.py` (growth ODE; $\varepsilon(a)$ family with kernel $p \in [4, 6]$; environment gate F_g ; reproduces the S_8 and ladder *illustrations*; documents priors/systematics).
- `referee_pipeline.py` (FRW averaging module; $\Omega_\Lambda = \beta f c_{\text{geo}}$ cross-check; computes toy $a_0 = (5/12)\Omega_\Lambda^2 c H_0$; generates `epsilon_evolution.png`).
- `fv_semi_analytic.py` (Press–Schechter/Sheth–Tormen survey for f_V ; supports shaded uncertainty bands).
- `gadget4_mu_eps_toy.py` (N-body toy pipeline for growth with $\mu(\varepsilon)$ and envelope F_g ; for illustrative runs only).
- `s8_hysteresis_run.py` (BAO toy χ_g sweeps; generates `bao_growth.png`).

Typical outputs include `epsilon_evolution.png` (Sec. VIII) and `bao_growth.png` (Sec. IX) for the illustrative runs. Scripts are annotated with usage notes. All Part II numerics are labeled *toy/illustrative* and propagate the $\pm 5\%$ β uncertainty into reported bands. Full Gadget-4 outputs will be added post-simulation.

SYMBOL INDEX

Symbol	Meaning
ℓ	Diamond radius (working order scale)
L_{curv}	Local curvature length
$\beta = 2\pi C_T I_{00}$	Modular-response sensitivity (QFT coefficient)
C_T	Stress-tensor two-point normalization (our convention)
I_{00}	Projected ℓ^4 integral coefficient (App. XV)
$\varepsilon(a)$	Dimensionless state variable from modular response
$\mu(\varepsilon)$	Growth coupling, $1/(1 + \frac{5}{12}\varepsilon)$
Σ	Lensing coupling (unity at working order)
$f c_{\text{geo}}$	Geometric/foliation factor (App. XVI)
κ	Local boost surface gravity, $\beta_{\text{KMS}} = 2\pi/\kappa$
T_{KMS}	Modular/KMS temperature, $\kappa/(2\pi)$
S_{sub}	Entanglement entropy variation in MI/moment-kill channel
α_{\log}	(Optional) marginal running: $\beta(\ell) = \beta_0[1 + \alpha_{\log} \ln(\ell/\ell_0) + \dots]$
χ_g	Geometric scalar, $\ell^2 \sqrt{C_{abcd} C^{abcd}}$
$F_g(\chi_g)$	Environment envelope
S_8	Growth amplitude observable
$\Omega_m(a)$	Matter fraction as a function of scale factor
Ω_Λ	Dark-energy density parameter

- [1] J. J. Bisognano and E. H. Wichmann, “On the Duality Condition for a Hermitian Scalar Field,” *J. Math. Phys.* **16**, 985 (1975); “On the Duality Condition for Quantum Fields,” *J. Math. Phys.* **17**, 303 (1976).
- [2] H. Casini, M. Huerta, and R. C. Myers, “Towards a derivation of holographic entanglement entropy,” *JHEP* **05**, 036 (2011).
- [3] H. Osborn and A. C. Petkou, “Implications of Conformal Invariance in Field Theories for General Dimensions,” *Annals Phys.* **231**, 311–362 (1994).
- [4] E. Bellini and I. Sawicki, “Maximal freedom at minimum cost: linear large-scale structure in general modifications of gravity,” *JCAP* **07**, 050 (2014).
- [5] L. Lombriser and A. Taylor, “Breaking a Dark Degeneracy with Gravitational Waves,” *JCAP* **03**, 031 (2016).

- [6] T. Jacobson, “Entanglement equilibrium and the Einstein equation,” *Phys. Rev. Lett.* **116**, 201101 (2016).
- [7] T. Faulkner, A. Lewkowycz, and J. Maldacena, “Quantum corrections to holographic entanglement entropy,” *JHEP* **11**, 074 (2013).
- [8] N. Lashkari, M. B. McDermott, and M. Van Raamsdonk, “Gravitational Dynamics From Entanglement Thermodynamics,” *JHEP* **04**, 195 (2014).
- [9] H. Araki, “Relative Entropy of States of von Neumann Algebras,” *Publ. Res. Inst. Math. Sci.* **11**, 809–833 (1976).
- [10] S. Hollands and R. M. Wald, “Local Wick Polynomials and Time-Ordered-Products of Quantum Fields in Curved Spacetime,” *Commun. Math. Phys.* **223**, 289–326 (2001).
- [11] C. J. Fewster and S. Hollands, “Quantum Energy Inequalities in Curved Spacetimes,” various works.
- [12] H. Casini and M. Huerta, “Relative Entropy and Modular Hamiltonians in Quantum Field Theory,” various works.
- [13] H. Casini, D. A. Galante, and R. C. Myers, “Comments on Jacobson’s ‘Entanglement equilibrium and the Einstein equation’,” *JHEP* **03**, 194 (2016), arXiv:1601.00528.